APPLICATION OF MESOPOROUS SILICA MATERIALS FOR THE IMMOBILIZATION OF POLYPHENOL OXIDASE

MASTER THESIS IN FOOD SCIENCE AND ENGINEERING
2013/2014

Author
Paula Corell Escuin
Supervisor
Dr. Alfonso García-Bennett
Directors
Dr. Ana María Andrés Grau
Dr. Ángel Luís Argüelles Foix

APPLICATION OF MESOPOROUS SILICA MATERIALS FOR THE IMMOBILIZATION OF POLYPHENOL OXIDASE

Paula Corell Escuin, Alfonso García-Bennett[1], Ana María Andrés Grau[2], Ángel Luís Argüelles Foix[2].

ABSTRACT

Enzymatic browning is one of the most important reactions that occur in fruits and vegetables, resulting in negative effects on color, taste, flavour and nutritional value. The main agent responsible for this reaction is polyphenol oxidase (PPO), also called tyrosinase, because it oxidises phenolic compounds and generates dark pigments. Mesoporous materials have been popular for a variety of applications in the last two decades, such as catalysis and gas separation, and they are an interesting option to immobilize the PPO as an alternative to the established industry process based on heat treatments. The objective of the present work is to study the possibility to remove this enzyme or even inhibit its activity from apple juice, since this beverage is rich in polyphenols and it is susceptible to suffering enzymatic browning. Different mesoporous silica materials were tested with different structures, morphologies and porosities in order to see their influence on the immobilization rate. Besides, the pH value of the solution and time were fully analysed and they provide results to obtain a good immobilization capacity. Pore volume, is the textural characteristic which affects the most the immobilization assay. Aeroperl® and SBA-15 are the materials which can adsorb larger quantity of PPO at pH 4.00, because electrostatic interactions can exist between the enzyme and the silica walls. Fitting power law and Higuchi models, we can assume that the PPO loading into mesoporous materials is diffusion controlled. The commercial mesoporous material reveals highest inhibition rates in real apple extracts.

KEYWORDS: mesoporous material, silica, tyrosinase, polyphenol oxidase, PPO, juice treatment, enzymatic browning.

[1]Department of Material and Environmental Chemistry (MMK), Stockholm University (SU) SE-106 91 Stockholm, Sweden.
[2]Instituto Universitario de Ingeniería de Alimentos para el Desarrollo (IUIAD-UPV). Universidad Politécnica de Valencia Camino de Vera, s/n 46022 Valencia. España.

RESUMEN

La principal reacción que afecta tanto a frutas como a verduras y que causa un detrimento en su color, sabor, olor y valor nutricional es el pardeamiento enzimático. La polifenol oxidasa (PPO), también llamada tirosinasa, es la principal responsable de esta reacción, ya que oxida los compuestos fenólicos generando pigmentos parduzcos. Los materiales mesoporosos han tenido una gran variedad de aplicaciones en las últimas dos décadas, como por ejemplo catálisis y separación de gases, y estos materiales son una interesante opción para inmovilizar la PPO como alternativa a los tratamientos térmicos implementados en la industria. El objetivo de este trabajo es estudiar la posibilidad de retener este enzima o incluso inhibir su actividad aplicándolo sobre zumo de manzana, puesto que, como esta bebida es rica en compuestos fenólicos, es más susceptible de sufrir esta reacción de pardeamiento. Para ello, se han estudiado diferentes materiales mesoporosos de sílice con diferentes estructuras, morfologías y porosidades para poder dilucidar su influencia en la tasa de inmovilización. Además, otros factores que han sido ampliamente estudiados han sido la influencia del pH de la solución de inmovilización y el tiempo de contacto entre el material y el enzima. La característica textural que parece ser decisiva en los ensayos de inmovilización es el volumen de poro. Aeroperl® y SBA-15 son los dos materiales que pueden atrapar mayor cantidad de PPO cuando la solución tiene un valor de pH de 4.00, puesto que a ese valor de pH pueden establecerse las interacciones electrostáticas necesarias para que el enzima pueda quedar adsorbido en las paredes del material. Ajustando los modelos de Higuchi y power law podemos deducir que el proceso de entrada de la PPO dentro de los poros está controlado difusionalmente. El material comercial testado es el que presenta mayores tasas de inhibición en extractos de manzana.

PALABRAS CLAVE: material mesoporoso, sílice, tirosinasa, polifenol oxidasa, PPO, tratamiento de zumos, pardeamiento enzimático.

RESUM

La principal reacció que afecta tant fruites com a verdures i que causa un detriment en el seu color, sabor, olor i valor nutricional és l'enfosquiment enzimàtic. La polifenol oxidasa (PPO), també anomenada tirosinasa, és la principal responsable d'aquesta reacció, ja que oxida els compostos fenòlics generant pigments terrosos. Els materials mesoporosos han tingut una gran varietat d´aplicacions en els últims 20 anys, com per exemple catàlisi i separació de gasos, i aquéstos són una interessant opció per a immobilitzar la PPO com a alternativa als tractaments tèrmics implementats en la industria. L'objectiu d´aquest treball és estudiar si és possible retindre aquest enzim o fins i tot inhibir la seua activitat aplicant-ho sobre suc de poma, ja que, com aquesta beguda és rica en compostos fenòlics, és més susceptible de patir aquesta reacció d'enfosquiment. En el present treball, s'han estudiat diversos materials mesoporosos de sílice amb diferents estructures, morfologies i porositats per a poder dilucidar la seua influència en la taxa d'immobilització. A més, altres factors que han sigut àmpliament estudiats han sigut el pH de la solució d'immobilització i el temps de contacte entre el material i la solució enzimàtica. La característica textural que sembla ser decisiva en els assajos d'immobilització és el volum de porus. Aeroperl® i SBA-15 són els dos materials que poden atrapar major quantitat de PPO quan la solució té un valor de pH de 4.00, ja que per a aquest valor de pH poden establir-se les interaccions necessàries perquè l'enzim puga quedar adsorbit en les parets del material. Ajustant el model de Higuchi i power law podem deduir que el procés d'entrada de la proteïna dins dels porus està controlat difusionalment. El material comercial testat és el que presenta majors taxes d'inhibició en extractes de poma.

PARAULES CLAU: material mesoporoso, sílice, tirosinasa, polifenol oxidasa, PPO, tractament de suc, enfosquiment enzimàtic.

INTRODUCTION

Since the early 90s, the development of novel mesoporous materials has been at the forefront of materials science. Consequently, they are expected to find applications in various industrial fields such as catalysis (Taguchi and Schüth, 2005), separation (Giraldo *et al.,* 2007), drug delivery (Vallet-Regi *et al.*, 2001) or even food technology (Pérez-Esteve *et al.*, 2013).

According to the International Union of Pure and Applied Chemistry (IUPAC) notation, microporous materials have pore diameters of less than 2 nm, the diameter of the pores in macroporous materials are larger than 50 nm and mesoporous materials have pore size between 2 - 50 nm. The latter have narrow pore size distributions, high surface areas and their pore sizes are comparable to the diameter of enzymes. This is the main reason why these materials have begun to attract attention as supports for enzyme immobilization (Wang and Caruso, 2005). Their synthesis using surfactant templates was discovered two decades ago by two independent groups: the group at Waseda University headed by K. Kuroda (Yanagisawa *et al.*, 1990) and the group working at Mobil Company headed by C.T. Kresge (Kresge *et al.*, 1992).

In general terms, the preparation of mesoporous surfactant-templated silicates, as it is shown in Figure 1, requires a silica source, a catalyst for silica polymerization, a surfactant template and a solvent, which is usually water. In essence, there are three main routes to synthesise ordered mesoporous materials. The first one was proposed from Kuroda´s work and it is called "Folded Sheet Mechanism" (FSM), name also given to the materials synthesised by this method. This mechanism is based on layered silicates, such as kanemite, inside which organic compounds are inserted in between the layers and then, by heating or ion exchange, the silica is condensed to form three-dimensional networks silicates (Inagaki *et al.* 1993). The second model is Liquid Crystal Templating (LCT) in which surfactants are initially forming structures called micelles followed by the migration and polymerization of the inorganic silicate species (Atluri, 2010). Finally, Evaporation-Induced Self-Assembly (EISA) where no micelles are present in solution at first, but where the concentration of the solution is increased by heating and evaporating the solvent, so that there is an instant when the surfactant concentration is high enough to form micelles and where the silicate can precipitate and create the mesoporous materials (Edler, 2011).
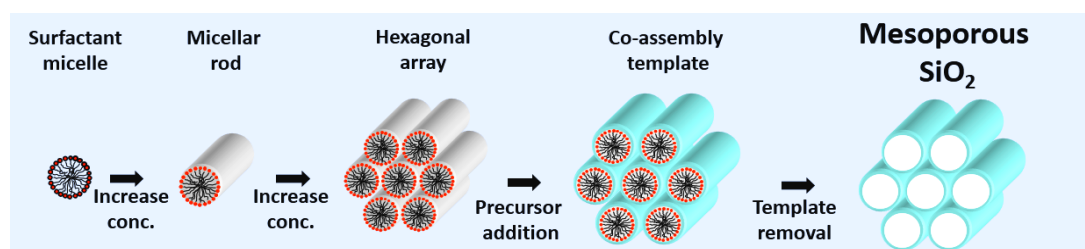
FIGURE 1. A general scheme for the synthesis mechanism of mesoporous surfactant-templated silicates.

Surfactants are chemicals that lower the surface tension of a liquid and lower also the interfacial tension between two liquids. A single molecule of a surfactant is composed by a hydrophilic and a hydrophobic part. Both of them are connected by a covalent bond. In solutions above a certain concentration, known as the critical micelle concentration (CMC), they arrange themselves at interfaces forming aggregates, also called micelles. These micelles are thermodynamically stable structures but, at the same time, dynamic. Their shape above the CMC can be an indication of the shape of the pore in the resulting inorganic mesoporous material which can be predicted by the packing parameter, $g = V/a_0l$. This parameter is related to the total volume of the surfactant chain, V, the effective headgroup area of the surfactant, a_0, and the kinetic surfactant tail length, l. Based on this definition, lamellar structures have a g value between ½ and 1, cylindrical ⅓ < g ≤ ½ and spherical g ≤ ⅓ (Han, 2010). Thus, micelles can produce different mesoscopic phases depending on the surfactant concentration and temperature. A diagram above the Krafft temperature (minimum temperature at which surfactants can form micelles) illustrating the most significant structures that can be formed by micelles is shown in Figure 2.
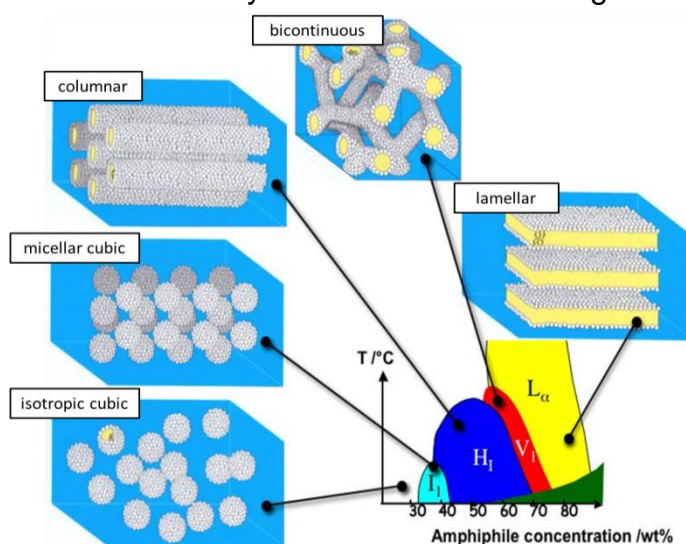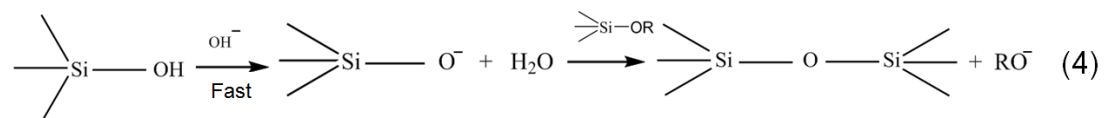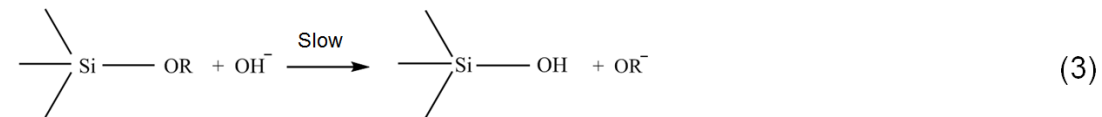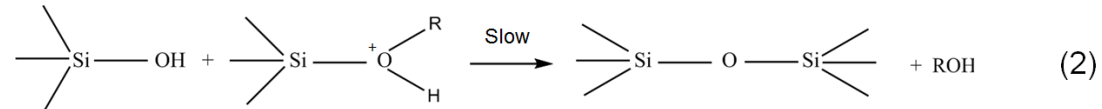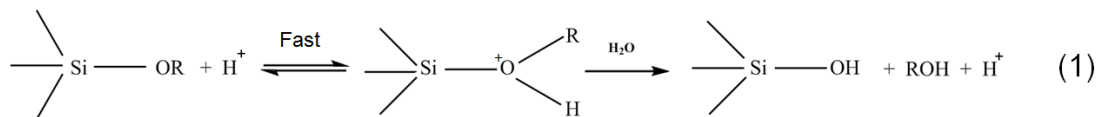

FIGURE 2. A schematic phase diagram showing the mesophases which can be formed depending on the concentration of the surfactant and the temperature.

Depending on the charge of the hydrophilic headgroup of the surfactant molecule, they can be classified as cationic (*e.g.* quaternary ammonium, Beck *et al.*, 1992), anionic (*e.g.* sulphate, Huang *et al.,* 2000), zwitterionic which means that the same molecule has a positive and a negative charge (*e.g.* amino acids, Yokoi *et al.* 2006) or neutral (*e.g.* amines, Tanev and Pinnavaia, 1995).

Larger self-assembled structures are obtained by using polymeric surfactants (*e.g.* Pluronic®, Bagshaw *et al.*, 1995). Small molecule surfactants, such as cetyltrimethylammonium bromide (CTAB) produce materials with pore size from 2 to 3 nm and can be controlled by altering the hydrophobic tail length of the surfactant. On the other hand, polymeric surfactants, such as triblock copolymer surfactants, can produce much larger pore diameters up to 30 nm (Zhao *et al.*, 1998).

As the silica condensation reaction can be done under acidic, alkaline or neutral conditions, it is very important to understand the characteristics of silica precursors under different conditions and at different pH values. The polymerization of silica precursors occurs via hydrolysis and condensation reactions. The detailed hydrolysis and condensation reaction mechanism under acidic conditions is described in equation 1 and 2 respectively. The same reactions but in alkaline conditions are represented in equations 3 and 4. As it is shown, the polymerization rate depends mainly on the pH of the solution. An acid solution enhances the hydrolysis more than condensation, while basic solutions do it the other way around. The most common silica precursors used for mesoporous silica synthesis are sodium silicate (Na_2SiO_3) and alkoxysilanes, such as tetramethyl orthosilicate (TMOS), tetraethyl orthosilicate (TEOS) and tetrapropyl orthosilicate (TPOS).

$$\equiv Si - OR + H^+ \underset{Fast}{\rightleftharpoons} \equiv Si - {}^+O\Big\langle{}^R_H \xrightarrow{H_2O} \equiv Si - OH + ROH + H^+ \qquad (1)$$

$$\equiv Si - OH + \equiv Si - {}^+O\Big\langle{}^R_H \xrightarrow{Slow} \equiv Si - O - Si\equiv + ROH \qquad (2)$$

$$\equiv Si - OR + OH^- \xrightarrow{Slow} \equiv Si - OH + OR^- \qquad (3)$$

$$\equiv Si - OH \xrightarrow[Fast]{OH^-} \equiv Si - O^- + H_2O \xrightarrow{\equiv Si - OR} \equiv Si - O - Si\equiv + RO^- \qquad (4)$$

Once the mesoporous silicates are formed, the surfactant template has to be removed. This is typically done by burning out the organic template at high temperatures (500-600°C) in a furnace under flowing air, nitrogen or sequentially nitrogen followed by an oxygen flow, all of them with temperature ramps of 1-2 ^{o}C·min^{-1}. Alternatively, the surfactant can be removed by solvent extraction.

The name of materials in this field is under review by the Mesoporous Materials Commission of the International Zeolite Association (IZA). Most of the surfactant-templated materials have been named by their discoverers using a series of three letters followed by a number. The letters refer to the university, company or research group that first published these materials and they have their internal numbering system.

Since the discovery of the first mesoporous material in the early 1990s, huge progress has been made in their synthesis, in the control of their pore characteristics, and solving the details of their inner structure. At the same time, potential applications of these materials have also been studied because of their ability to provide space for functional groups on the silica

wall. Mesoporous silica materials possess a high density of silanol groups after the removal of the template by calcination. This feature provides numerous possibilities for selecting these materials as carriers, adsorbents and supports, or for further reactions with organic functional groups.

Apples (*Malus domestica*) are one of the most important sources of polyphenols (phenolic compounds) in the human diet (Hertog *et al.,* 1992) and a classic example of fruit susceptible of enzymatic browning, which is a major problem for the fruit processing industry (Coseteng and Lee, 1987). Several studies have shown that enzymatic browning in apple pulp is associated with its polyphenol content (Murata *et al.,* 1995) and/or polyphenol oxidase activity (Walker, 1964). The Enzyme Commission (EC) classifies this enzyme (EC number 1.10.3.1) inside the group of Oxidoreductases because it acts in diphenols as oxygen acceptor.

The polyphenol oxidase (PPO), also known as tyrosinase, phenolase, catechol oxidase, *o*-diphenoloxidase, monophenol oxidase, laccase and creolase because of its activity, was first discovered and isolated in mushroom. This is the main reason why it is used as a model. This enzyme can act on two types of substrates: monohydroxyphenols (*e.g.* p-cresol) and *o*-dihydroxyphenols (*e.g.* catechol). The first type are hydroxylated into *o*-phenols and the other group are oxidized forming their corresponding quinones. These quinones are then polymerized with other quinones or phenolics, creating brown pigments, see Figure 3.

The control of enzymatic browning is of great importance to the horticulture industry, because this reaction occurs in many fruits and vegetables, often negatively affecting the attributes of color, taste, flavour, and nutritional value. It is estimated that more than 50% of the fruit market losses are a result of enzymatic browning (Whitaker and Lee, 1995).
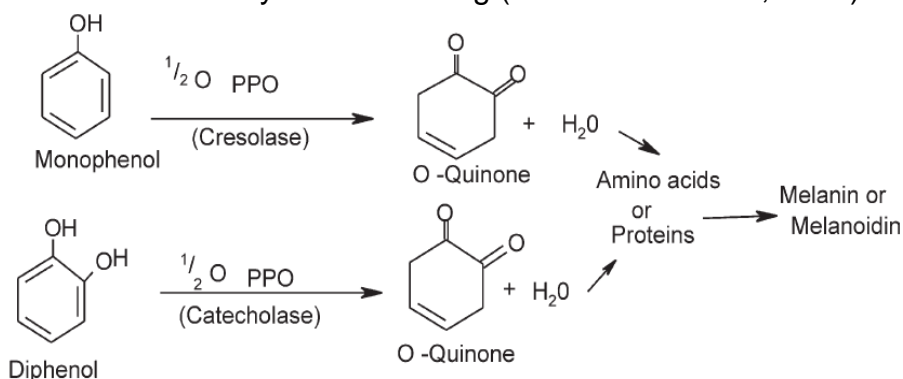
FIGURE 3. A generalized reaction mechanism for plant PPO (Gacche *et al.* 2003).

Several methods have been proved for the inhibition of PPO activity in fruit and vegetables. Sulphites have been used as agents to prevent browning, but also have been associated with severe allergies in certain vulnerable populations, restricting their application in food and beverages (Sapers, 1993). Heat treatments are unsuitable for inhibit such reactions, due to the detriment in nutrient and vitamin content or as it can even induce more browning reactions (Toribio and Lozano, 2006). Whereas, the addition of ascorbic acid has been a good alternative to the use of sulphites or other

chemical agents (Denoya *et al.* 2012; Gacche *et al.* 2003), anoxic conditions (Rocha and Morais, 2001), refrigeration and non-thermic treatments (Perez-Gago *et al.* 2006; Olivas *et al.* 2007) have also shown good results, despite their industrial application being less developed.

The physicochemical properties of mesoporous materials make them suitable candidates for the specific immobilization or inhibition of this enzyme. There are several studies already immobilizing enzymes (Arroyo, 1998; Datta *et al.*, 2013, Kupferschmidt *et al.* 2014), but only a few of them are made with PPO and mesoporous materials. Concretely, their purpose is far from the food industry, as they entrap PPO to detect phenolic compounds (Mangrulkar *et al.*, 2012) or to produce *o*-diphenols *in vitro* (Marín-Zamora *et al.*, 2009).

The aims of this thesis are to select and to characterize a wide variety of mesoporous materials suitable for encapsulating enzymes. Once their attributes are known, the possibility of immobilizing or sequestrating polyphenol oxidases from a model solution, only containing buffer and a commercial enzyme, was tested. In this part of the study, we also measured the influence of pH value and the textural characteristics of the materials on the immobilization rate. Finally, we wanted to examine the best materials into real apple extracts in order to elucidate their potential application in the juice industry.

MATERIALS AND METHODS

Materials

The chemicals sodium hydroxide (NaOH), potassium phosphate monobasic (KH_2PO_4), PPO from mushroom lyophilized powder 3130 units·mg^{-1} solid, Bradford Reagent, Bicinchoninic Acid solution and Copper (II) sulfate solution 4% (w/v) were purchased from Sigma-Aldrich and used as received. And hydrochloric acid (HCl) 37% and pure water (HiPerSolv CHROMANORM) were purchased from VWR PROLABO® Chemicals.

All laboratory procedures took place at the Laboratory of Material and Environmental Chemistry Department, Stockholm University, Sweden, with the exception of the measurement of PPO activity with apple extract, which was carried out at the Institute of Food Engineering for Development (IUIAD-UPV), Polytechnic University of Valencia, Spain.

Methods

MESOPOROUS SILICA MATERIALS

Various mesoporous silica materials were tested in this study having different textural characteristics in order to compare their ability to immobilize PPO enzyme. These materials are: SBA-15 (University of California at Santa

Barbara), SBA-3 (University of California at Santa Barbara), MCM-48 (Mobil Crystalline Materials), STA-11 (University of St. Andrews) and Aeroperl® 300/30 (commercial material purchased from Evonik Industries). The following table (Table 1) summarizes their synthesis conditions and their structures.

TABLE 1. Synthesis details and pore structure of the mesoporous materials used in this study.

Material	Silica source	Surfactant	Conditions	Structure	Reference
Aeroperl®	Fumed silica	Non applicable	Acidic	Disordered	Evonik Industries
SBA-15	TMOS	P123®	Acidic	2D hexagonal	Zhao *et al.* 1998
SBA-3	TEOS	CTMABr	Acidic	2D hexagonal	Anunziata *et al.* 2007
MCM-48	TEOS	CTMABr	Basic	3D bicontinuous cubic	Wang *et al.* 2001
STA-11	TEOS + MPTES	P123®	Acidic	3D bicontinuous cubic	Hodgkins *et al.* 2005

CHARACTERIZATION TECHNIQUES

Low angle X-ray powder diffraction (XRD)

XRD is a fundamental technique to determine the atomic and molecular structure of a crystal. This is used in this work to determine if the material synthesised is ordered or not, and also the mesophase structures. Low angle XRD patterns presented were collected using the powder diffractometer PANalytical X´Pert PRO (PANalytical Corp., Almelo, the Netherlands) using CuKα radiation (λ = 1.5418 Å) at 45 kV and 40 mA. The diffraction patterns were recorded between 0.5° and 6°. For the 2D hexagonal structure the unit-cell parameter, *a*, was calculated according with the equation 5:

$$a = d \sqrt{\frac{4}{3} (h^2 + hk + k^2)} \tag{5}$$

where *d* is the interplanar distance and *h* and *k* the indexes denoting a plane orthogonal to the direction. In this case, as the material is two dimensional, (10) is the plane orthogonal to the direction *h*.

Scanning electron microscopy (SEM)

Scanning electron microscopy (SEM) is used to study the morphology and topography of the particles and their surfaces as well as to know their particle size. All the SEM images were obtained by JEOL JSM-7401F SEM operating at an accelerating voltage of 1.4-1.5 kV without sputtered coating and with a magnification of x 9,000. And the particle size is calculated from the SEM images with ImageJ, a program of digital image processing developed at the National Institutes of Health, US.

Transmission electron microscopy (TEM)

Transmission electron microscopy (TEM) provides the structural information of the sample in atomic scale using a high-energy electron beam. TEM is used in this study to determine the pore structure of the mesoporous silica particles and their symmetry, complementing low angle XRD information. In this case, TEM images were collected using a JEOL-3010 microscope, operating at 300 kV (C_s 0.6 mm, resolution 1.7 Å). Images were recorded using a CCD camera with specialized imaging shadow-graph (SIS) analysis (size = 1,024 x 1,024 megapixels, pixel size = 23.5 x 23.5 µm; model: Keen View, Olympus Soft Imaging Solutions, Munster, Germany) using low-dose conditions on calcined samples.

Nitrogen adsorption/desorption isotherms

Gas adsorption is the most practical and reliable method to determine the porosity of materials. The textural information of a solid material including surface area, pore volume and pore size distribution can be given by the adsorption of gases in a porous solid at various relative pressures and fixed temperature. The porosity information can be calculated from the nitrogen adsorption isotherm curves, the surface area is given by the amount of gas molecules needed to cover the surface with a complete monolayer based on the Brunauer-Emmett-Teller (BET) theory developed in 1938 (Brunauer *et al.*, 1938), the total pore volume is obtained by the amount of gas adsorbed at the relative pressure close to 0.94 from adsorption and the calculation of pore size distribution in this study is based on Density Functional Theory (Lastoskie *et al.* 1993). Nitrogen adsorption/desorption isotherms were measured at liquid nitrogen temperature (-196 °C) using a Micrometrics ASAP 2020 volumetric adsorption analyser.

Thermogravimetric analysis (TGA)

After 24 hours of immobilization, the enzyme solution was filtered with a 42 filter paper Whatman™ Cat No 1442-070 in order to remove the mesoporous material from the protein solution. Then, the material was analysed with a Perkin Elmer TGA 7 instrument with a ramp temperature between 30 and 900 °C and a nitrogen gas flow of 20 mL·min^{-1}. The weight measurement was registered against the temperature while the protein incorporated into the pores of the material was decomposed. TGA was used in this study to verify the real amount of PPO immobilized inside the mesoporous material.

In vitro IMMOBILIZATION ASSAYS

For the immobilization assays, commercial PPO from mushroom was used as an enzyme model before testing the materials with real apple extracts. Knowing the total pore volume of each material and the molecular weight of this enzyme (calculated from its aminoacid sequence), the mean volume of one molecule of enzyme is deduced ($3.18 \cdot 10^{-19}$ cm^3). Comparing

this calculation with the data reported in previous articles (Lü *et al.,* 2010; Sendovski *et al.,* 2011) and in BRENDA database, the concentration of PPO solution was established to 0.7 mg·mL^{-1}. Therefore, 7 mg of enzyme lyophilized was dissolved into 10 mL of phosphate buffer solution 50 mM at different pH values (1.00, 3.00, 4.00, 5.00 and 7.00).

The purpose of varying the acidity of the solutions is to study the effect of the pH in the immobilization rate. Each solution was added to 10 mg of each material separately with light agitation at room temperature. Samples were taken out at different times: 0, 15, 30, 60, 120, 360 and 3600 min and their protein concentration were measured by Bradford (Bradford, 1976) and Bicinchoninic Acid also called BCA (Smith *et al.,* 1985) methods in order to see the kinetics of the immobilization process. The measurement was done by triplicate for the five mesoporous materials tested but the standard deviation was never higher than 0.03. The absorbance measurements were obtained from a Perkin Elmer Lambda 19 UV/VIS/NIR spectrometer in 2 mL plastic cuvettes.

In situ ACTIVITY ASSAYS

Apple extracts were obtained from Granny Smith cultivar apples purchased in a local supermarket (Mercadona, Spain). The extracts were obtained according to the method proposed by Guerrero 2009. 20 g of chopped apples, after peeling and core removal, were homogenised with 80 mL of phosphate buffer 10 mM pH 7.0 using a dispersing machine ULTRA-TURRAX®. The slurry was filtered, treated with ammonium sulfate reagent ((NH_4)$_2$$SO_4$) 20 % p/p and then centrifuged 10.000x g for 20 min. The pellet was re-dissolved in phosphate buffer 50 mM pH 7.00. This procedure was done in duplicates.

The protein content in each extract was determined by Bradford method (Bradford, 1979) comparing with a standard curve, obtained previously, with different known concentrations of bovine serum albumin (BSA) protein.

The initial PPO activity of each extract was determined by spectrophotometric methods. The reaction mixture consisted of 1 mL of phosphate buffer pH 4.0 10 mM; 0.25 mL of extract and 0.25 mL of dopamine 0.03 mM as a substrate. The absorbance was registered during 2 min in a wavelength of 420 nm. One unit of enzymatic activity was defined by U = 0,001 ΔAbs_{420}·min^{-1}·(mL of extract)$^{-1}$ (Guerrero, 2009).

The same procedure was followed simulating the same immobilization assays as described before but instead of measuring the protein concentration of the solution at the different times as exposed before, what was recorded in this case is the PPO activity at different times (0, 15, 30, 45, 60 min) and only testing the best two materials which presented the highest immobilization rate: Aeroperl® and SBA-15 against a material which presented the lowest immobilization rate: STA-11, as a negative control.

RESULTS AND DISCUSSION

CHARACTERIZATION OF MESOPOROUS SILICA MATERIALS

Low angle X-ray powder diffraction (XRD)

Low angle X-Ray diffraction is used here to investigate the pore structure of the mesoporous materials. The incident X-Ray radiation produces peaks at certain scattering angles and gives a diffraction pattern, which contains the structural information of the sample. Figure 4 contains the diffractograms of a sample of SBA-15 and SBA-3 showing (10), (11) and (20) diffraction peaks consistent with a 2D hexagonal structure. The periodicity of the pores gives peaks between 0.5° and 6° (2θ). These kind of mesostructures can be described by conventional space group symmetries, but the structure determination of mesoporous materials is difficult to solve due to insufficient diffraction peaks. Transmission Electron Microscopy (TEM) is a useful complementary technique to solve detailed structure analysis.
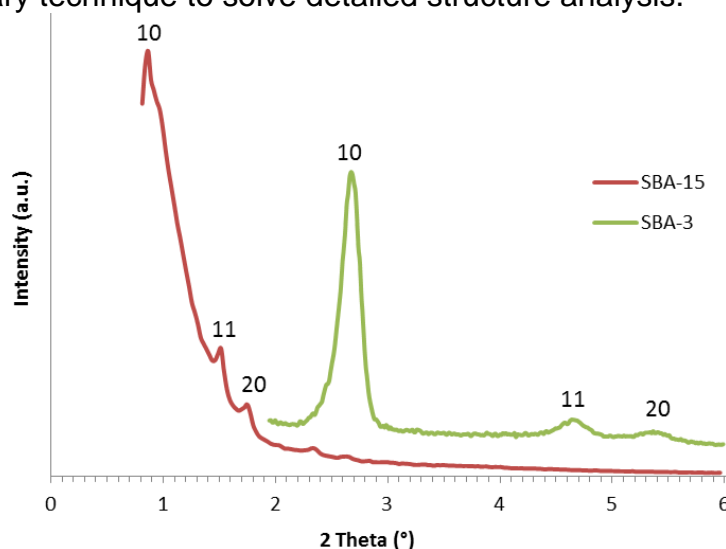

FIGURE 4. Low angle X-Ray diffraction patterns of SBA-15 and SBA-3 as examples of ordered mesoporous silica materials.

The unit-cell of these two materials was calculated according with the equation 5 presented in Materials and Methods and the results are for SBA-15 the unit-cell is 123.4 Å and for SBA-3 is 38.1 Å.

Scanning electron microscopy (SEM)

In this work knowing the textural and morphological characteristics of the materials are essential to understand their behaviour during the immobilization and activity assays. As it is shown in Figure 5, different morphological structures were chosen for this study. The SBA-15 particles used (Figure 5.A) have its typical single hexagonal plate-like structure (Zhao *et al.* 1998) with a particle size of 1.3-1.5 µm. SBA-3 particles (Figure 5.B) have a slightly amorphous morphology, elongated and convoluted at the same time. SEM was not a suitable technique to measure the particle size of SBA-3 due to from SEM particles are larger than 5 µm. Dynamic Light Scattering (not conducted) would have been a better technique for this

material. By contrast, the MCM-48 particles (Figure 5.C) are smaller and more aggregated (Schumacher *et al.* 2000) than any other material used in this work, with a particle diameter of less than 0.2 μm. Finally, STA-11 particles (Figure 5.D) are spherical and with a diameter between 2.00 and 2.80 μm. The commercial material used in this study, Aeroperl®, is spherical also, but its particle size is much bigger than the previous one, around 40 μm (picture not shown).
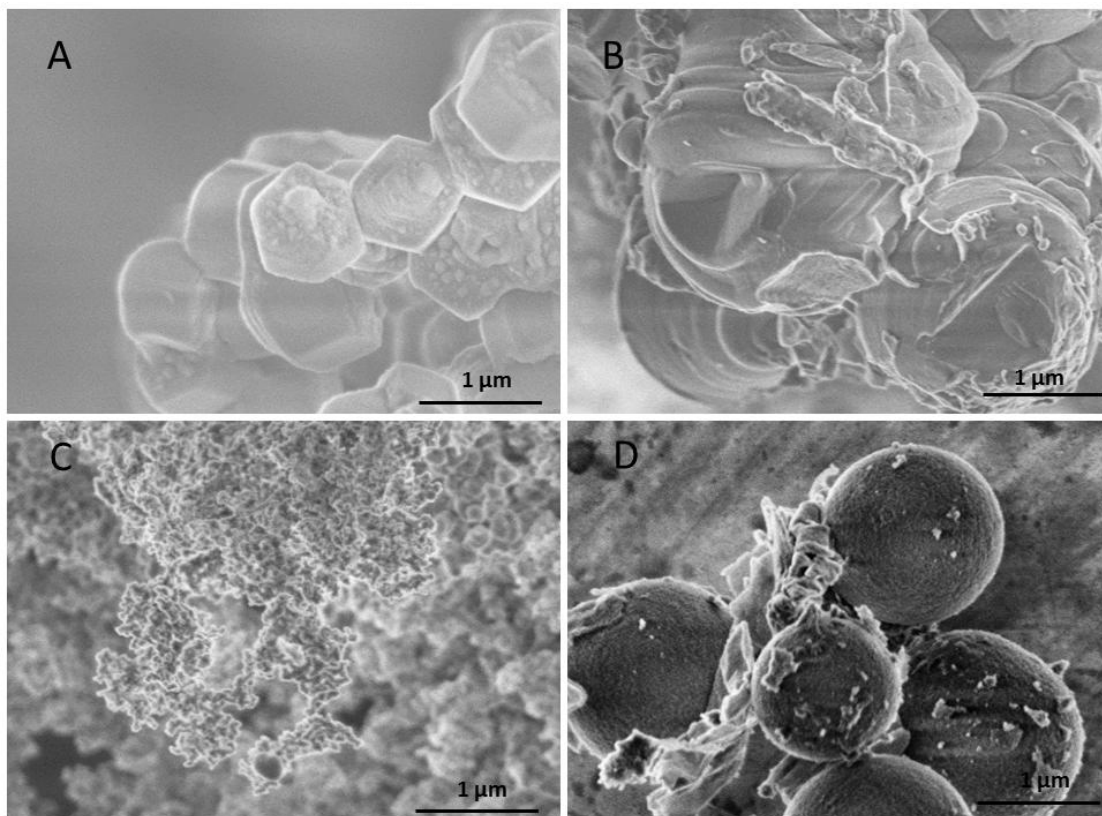

FIGURE 5. Scanning electron microscopy (SEM) images of mesoporous silica material calcined samples. **A.** SBA-15. **B.** SBA-3. **C.** MCM-48. **D.** STA-11.

Transmission electron microscopy (TEM)

In order to determine the pore structure of the materials, TEM images were obtained. Figure 6 shows differences between each type of mesoporous material, not only in their pores structure and symmetry but also in their wall thickness. The micrograph of STA-11 (Figure 6.A) was recorded with an incidence beam parallel to the (111) orientation. It shows its bicontinuous cubic structure with 3D-cylindrical pores. Its symmetry is cubic because if the crystal is seen along (111) orientation, its shape is hexagonal as it is shown in the Figure 6.A.

Figure 6.B and 6.D are showing the same structure (2D-hexagonal) along the same orientation (001) they belong to SBA-15 and SBA-3 respectively. The two of them have the same structure but they differ in their textural characteristics. Finally, Figure 6.C belongs to an amorphous material, as any symmetry and geometry can be found.
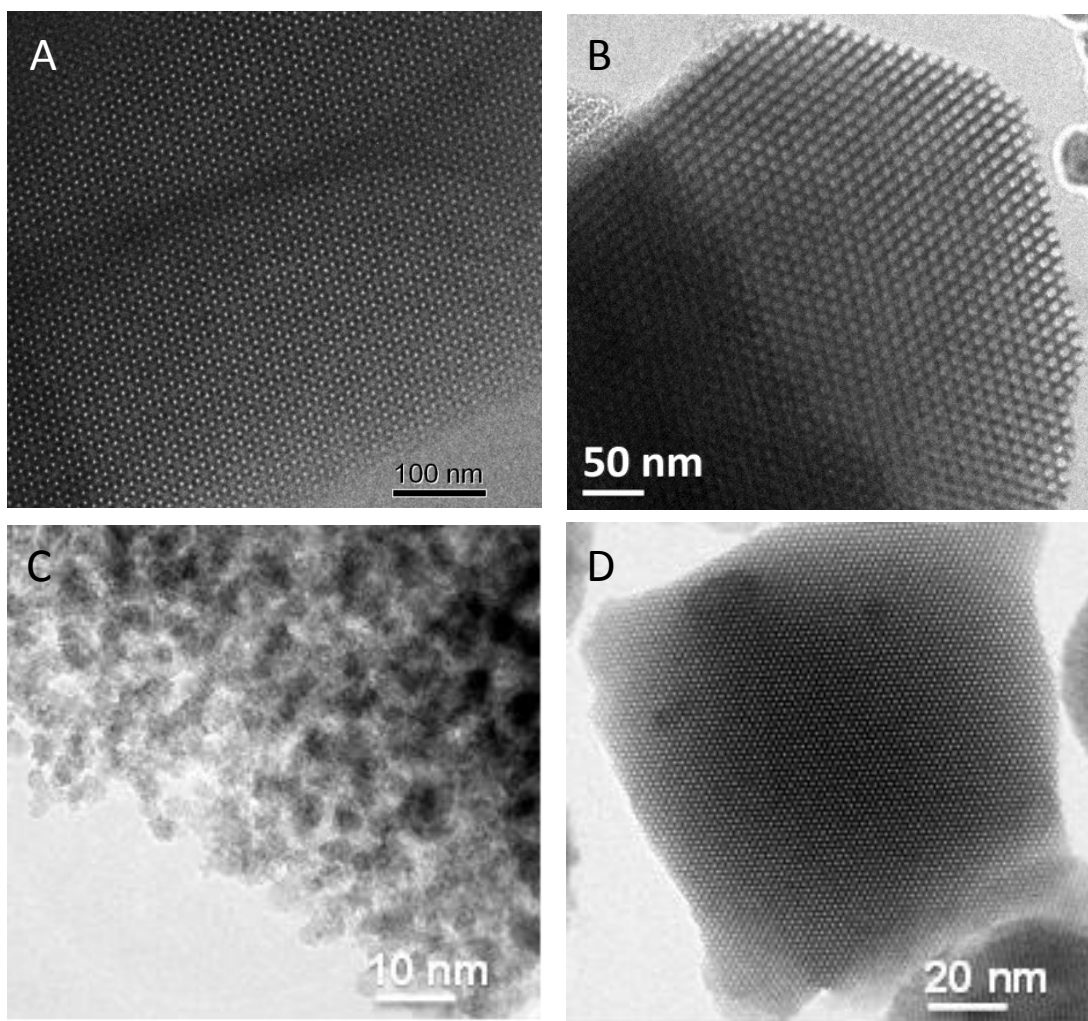
FIGURE 6. TEM images of mesoporous materials showing their pore structure and symmetry. **A.** SBA-11 (111). **B.** SBA-15 (001). **C.** Aeroperl® **D.** SBA-3 (001).
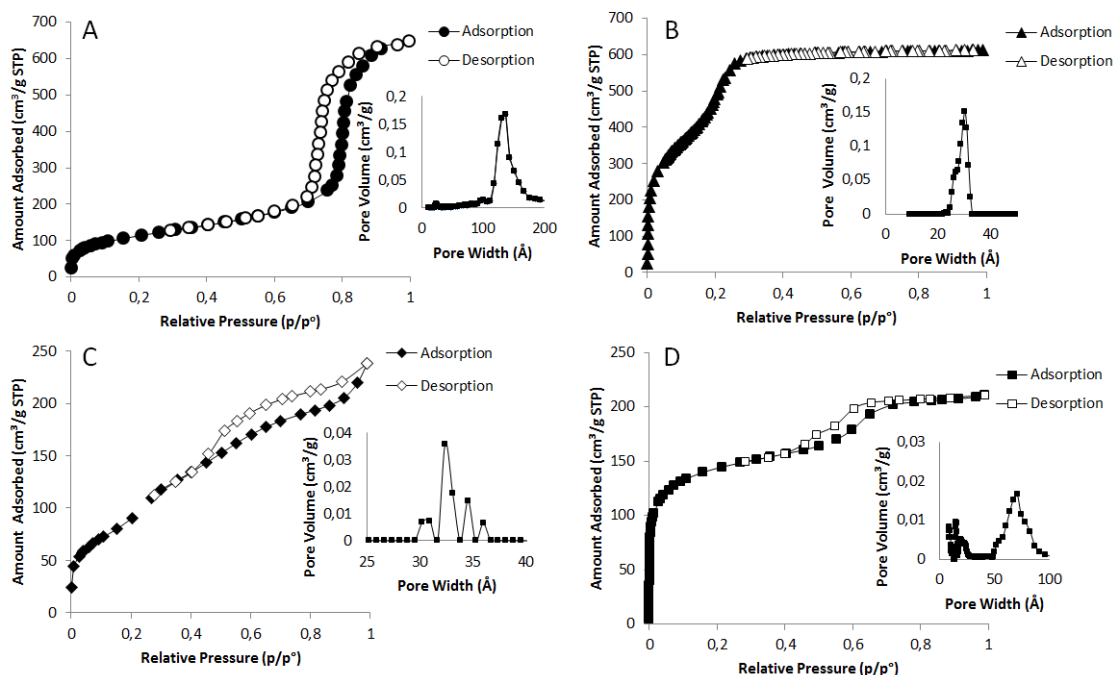
Nitrogen adsorption/desorption isotherms

In order to obtain more detailed information about the textural properties of the particles, a porosimetry analysis based on nitrogen adsorption/desorption isotherm was performed and the results are shown in Figure 7 and Table 2.

Each nitrogen isotherm has a typical type IV shape, according to the IUPAC classification, and also shows a sharp increase of nitrogen due to capillary condensation. The position of this uptake is shifted to higher relative pressures for SBA-15, indicating a larger pore size (see Table 2).

Apart from isotherms, hysteresis can also provide much important information about the pore structure. Each of the materials evaluated shows hysteresis, except for SBA-3 (Figure 7.B). SBA-15 (Figure 7.A) and STA-11 (Figure 7.D) show hysteresis type 1 whereas MCM-48 (Figure 7.C) has hysteresis type 4 according to IUPAC classification. If a material has hysteresis type 1 typically means that it has high pore-size uniformity, confirmed also by isotherm shape. By contrast, if the material has a type 4 hysteresis, it typically means that the material has a bimodal or cage-type

porous structure which in MCM-48 may arise from the small interparticle spaces.

Also note that the first two isotherms shown (from SBA-15 and SBA-3 respectively) has different scale than the other two which is explained according to the data in Table 2 where we can appreciate that their pore volume is much higher than the pore volume of MCM-48 and STA-11.

FIGURE 7. Nitrogen adsorption/desorption isotherm curves of calcined mesoporous materials used. Inserts show pore size distributions of each material derived from DFT-model assuming cylindrical pore geometry. **A.** SBA-15. **B.** SBA-3. **C.** MCM-48. **D.** STA-11. Note: solid symbols represent adsorption isotherms whereas open symbols plot desorption isotherms.

Regarding the pore size distribution shown in Figure 7, all of the materials have a narrow pore size distribution. According with the pore size calculated from Density Functional theory (DFT) – data shown in Table 2 – Aeroperl® has a wide range of pore width (80 – 300 Å). SBA-15 possesses an unusual large pore size (133 Å). SBA-3 shows the smallest pore size (29.2 Å) and MCM-48 and STA-11 are lying in between with a pore size of 33.4 Å and 66.8 Å respectively. The microporosity was calculated from t-plot analysis and the results are shown in Table 2. The only two materials which have microporous are SBA-15 and STA-11. The latter shows two different pore sizes in the microporous range (10.6 Å and 20.0 Å), apart from its mesoporous.

Another interesting aspect from Table 2 is that despite its low pore volume, SBA-3 has the biggest surface area due to its small pore size and unit cell. In contrast, Aeroperl®, the material with the biggest pore volume and pore size, has the smallest surface area of all of them. With this information we can conclude that pore volume and surface area have not always a positive correlation.
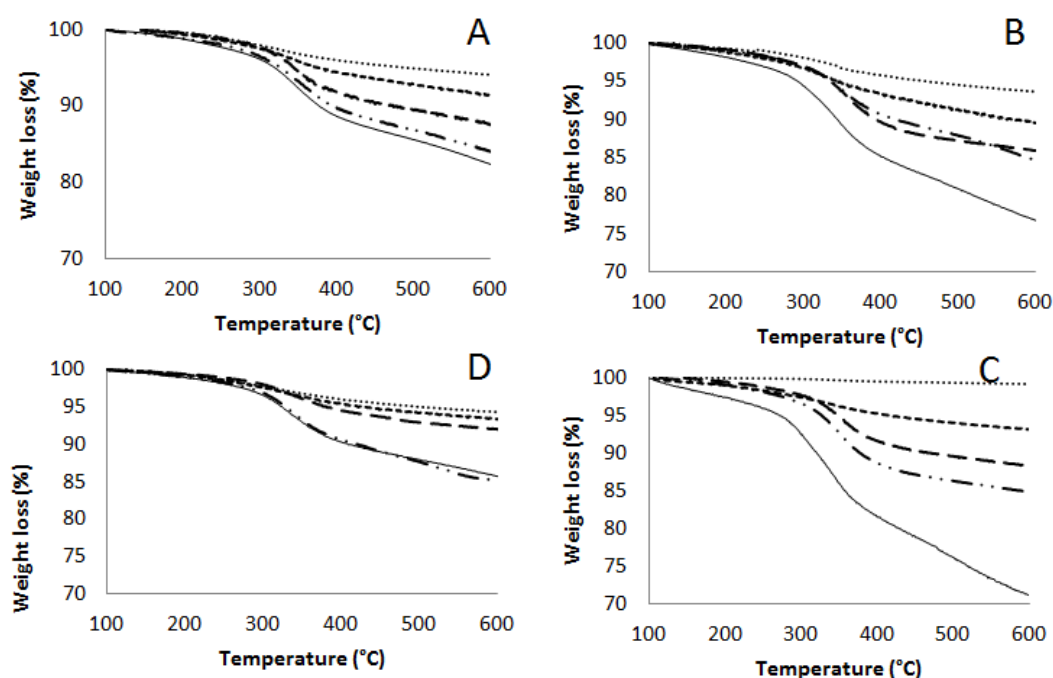
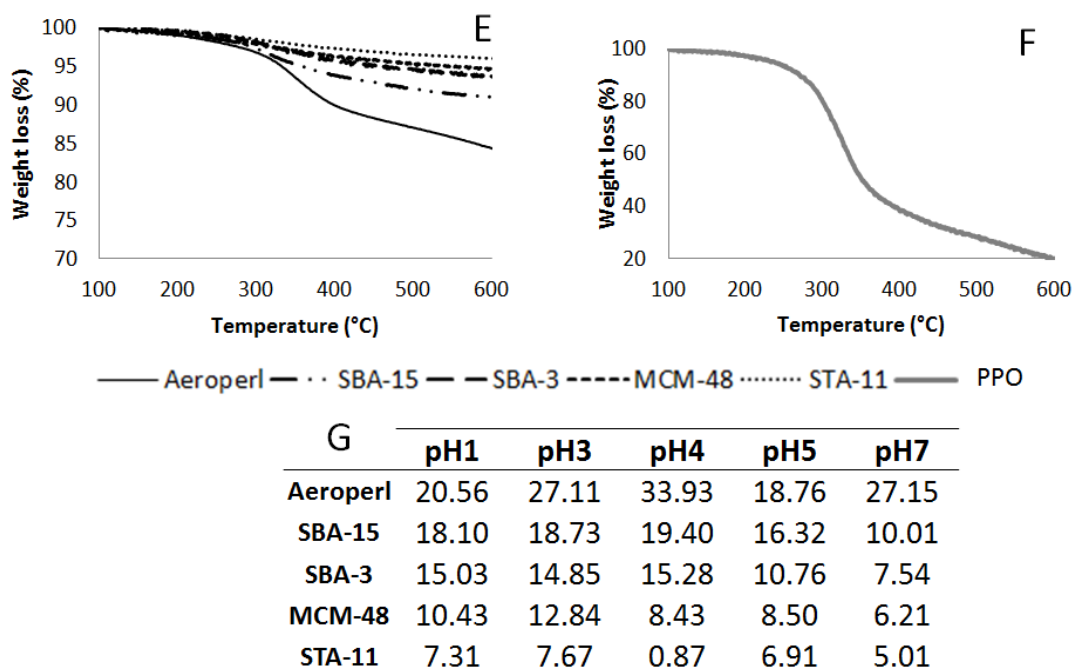**TABLE 2.** Pore structure parameters of mesoporous materials calculated from nitrogen adsorption data.

Material	Surface Area[a] (m^2/g)	MESOPOROUS		MICROPOROUS		
		Pore Volume (cm^3/g)	Pore size[b] (Å)	Pore Volume[c] (cm^3/g)	Surface area[c] (m^2/g)	Pore size[b] (Å)
Aeroperl®	237.3	1.6	80 - 300	-	-	-
SBA-15	411.8	1.00	133.0	0.023	66.3	25.2
SBA-3	1238	0.94	29.2	-	-	-
MCM-48	311.5	0.36	33.4	-	-	-
STA-11	529.5	0.32	66.8	0.14	178.9	20.0 / 10.6

[a] Surface area based on the Brunauer-Emmett-Teller (BET) theory. [b] Pore size derived from Density Functional Theory (DFT) model assuming cylindrical pore geometry. [c] Microporous parameters calculated from t-plot.

Thermogravimetric analysis (TGA)

All the results from the thermogravimetric measurements are collected in Figure 8. The mesoporous material filtered and dried after the immobilization were analysed by TGA instrument and each result was compared with the TGA result of the free PPO (Figure 8.F). These results show clear evidence that the pH value influences the immobilization rate as well as the pore volume. Materials with large pore volume can immobilize more quantity of PPO into their pores than the others. Thus, Aeroperl® shows higher percentage of weight loss in TGA than the rest of the materials in all the pH values. As the pore volume is smaller, the quantity of enzyme immobilized is also smaller. Besides, for all the materials studied, the pH value which shows higher percentage of PPO immobilized is pH 4.00 – except for the MCM-48 – because of the electrostatic interactions that can exist between silica walls and PPO. The amount of PPO retained into the pores can reach up to 30% of the weight of the material in the case of Aeroperl® at pH 4.00, whereas at the same pH value STA-11 retains almost no enzyme (less than 1%).

G	pH1	pH3	pH4	pH5	pH7
Aeroperl	20.56	27.11	33.93	18.76	27.15
SBA-15	18.10	18.73	19.40	16.32	10.01
SBA-3	15.03	14.85	15.28	10.76	7.54
MCM-48	10.43	12.84	8.43	8.50	6.21
STA-11	7.31	7.67	0.87	6.91	5.01

FIGURE 8. Thermogravimetric weight loss curves of each material after the immobilization assay. **A.** pH value 1.00. **B.** pH value 3.00. **C.** pH value 4.00. **D.** pH value 5.00. **E.** pH value 7.00. **F.** Free PPO. **G.** Table containing all the percentages of weight loss for each material at the different pH values.

In vitro IMMOBILIZATION ASSAYS

Knowing the textural and morphological properties of the materials tested allows for understanding the results of the immobilization assays (Figure 9). The amount of enzyme immobilized shown was determined using the Bradford method. Data collected by Bicinconinic Acid (BCA) method were inconsistent. One possible explanation for this is that the BCA method has a linear response in low protein concentration solutions according to the SIGMA specifications (Catalog Numbers BCA1 and B9643), and the concentration used in this assays is 0.7 mg·mL^{-1}. Thus, this method is more accurate for protein solutions less concentrated than the one used for the immobilization assays in this work. Error bars do not appear in the figures because they are too small (standard deviation less than 0.03 in all the measurements).

It is easily observed that each material tested has a different behaviour against the immobilization but all of them present higher rate at pH 4.00. One possible reason is because the silanol groups of mesoporous walls are charged negatively at this concrete pH value and the PPO, which has a pI value around 5.0 (Fan and Flurkey, 2004), is charged positively. Electrostatic interactions can exist between the enzyme and the silica wall and it can be immobilized or at least adsorbed.

The other two pH values tested near from this value (pH 3.00 and 5.00) also present high immobilization rate, around 200 mg·g^{-1}. By contrast, the

solutions far from the pH value were these two components are charged oppositely (pH 1.00 and 7.00) show almost no PPO immobilized - less than 100 mg of PPO per g of mesoporous material -. Because at pH 1.00, the silanol groups of the silica walls are charged positively ($SiOH_2^+$) and the enzyme also; whereas at pH 7.00 both enzyme and silanol groups have a charge negative.

These differences between the quantities of PPO immobilized at the different pH values are more noticeable in materials with high pore volume such as Aeroperl® or SBA-15. These same materials, with higher pore volume and pore size, also exhibit high amount of enzyme adsorbed. This is due to their larger pore size; PPO can diffuse more easily and is freer to interact with the silanol groups of the silica walls than in materials such as MCM-48 or STA-11 which have narrow pore diameters.

Another interesting aspect shown in Figure 9 is the influence of the immobilization time. Giving more time to interact the enzyme with the mesoporous materials benefits the PPO to be immobilized on the silica walls. Furthermore, the amount of enzyme adsorbed after 15 min in materials with larger pore diameters (Aeroperl® and SBA-15) remains constant. It happen for all the pH values except for pH 5.00 that it seems to need more time to reach the maximum quantity of PPO adsorbed.
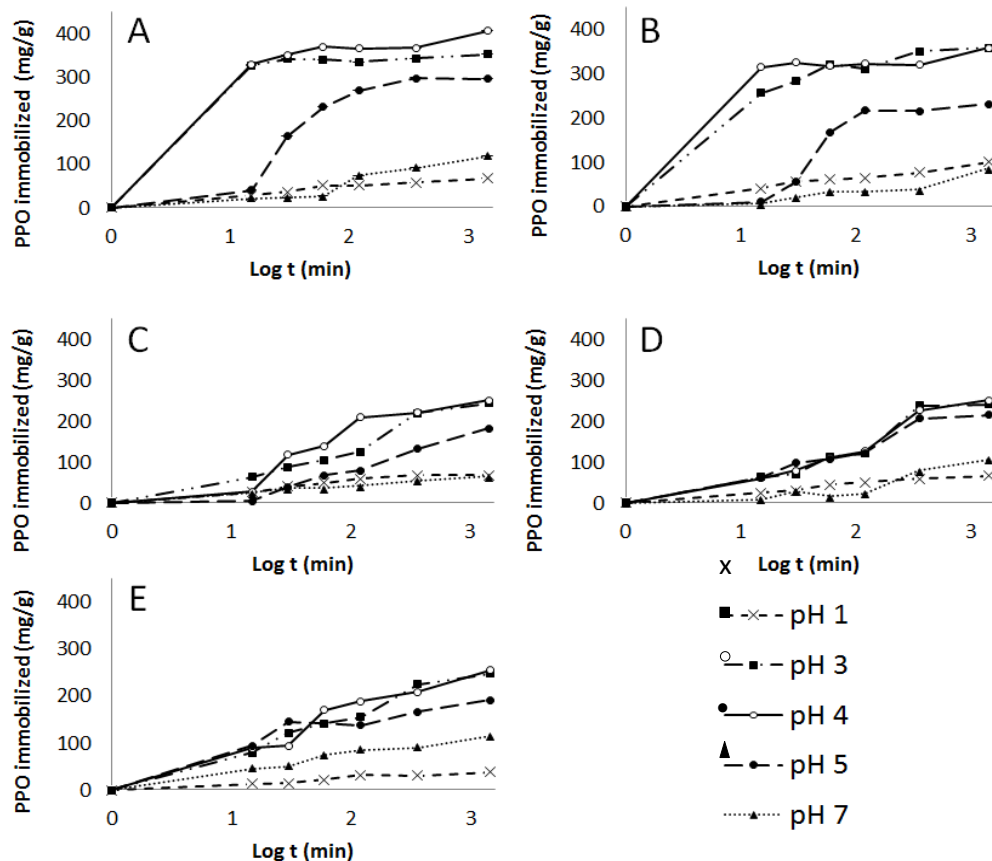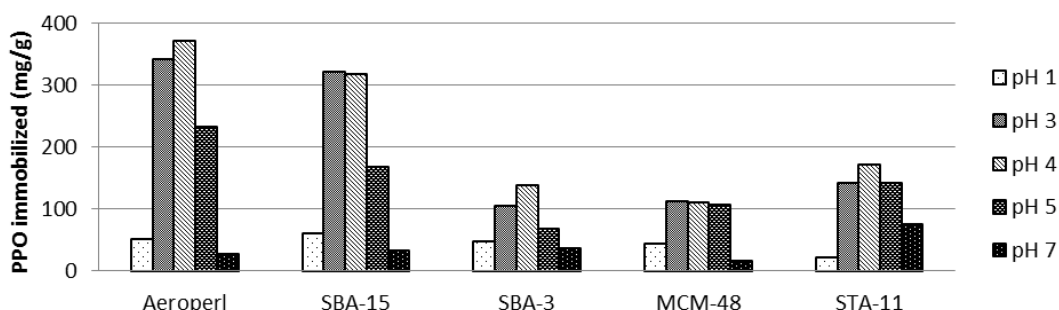

FIGURE 9. Immobilization kinetics of PPO (mg of enzyme / g mesoporous material) into the different materials at different pH values. **A.** Aeroperl® **B.** SBA-15 **C.** SBA-3 **D.** MCM-48 **E.** STA-11.

In order to understand the influence of the pH value in the immobilization rates of each material better, the same results were plotted in a new graphic

but only showing one measure of time - after 60 min of immobilization - and all the pH values were compared in the same graphic, these results are shown in Figure 10.

Materials having higher pore volume and bigger pore size can immobilize more PPO than those with low pore volume and size. On the other hand, for the first two materials, Aeroperl® and SBA-15, the pH value has more influence on the immobilization ability than the other three materials. The pH value of 4.00 results higher amount of PPO adsorbed for all materials, followed closely by a pH value of 3.00. The pH value which shows the minimum quantity of enzyme immobilized is pH 7.00, except for the STA-11 material. It is noticeable that Aeroperl® and SBA-15 need less time to immobilize high levels of PPO. After only 1 hour of contact both materials reach the maximum quantity of enzyme adsorbed (also observed in Figure 9).

FIGURE 10. Amount of PPO adsorbed (mg of enzyme / g of mesoporous material) into the different materials at different pH values after 1 hour of immobilization assay.

At this stage, with the results presented so far, it is clear that the material studied retain different amount of PPO depending on the pH value and their textural properties.

Furthermore, all the kinetic curves were fitted by power law and Higuchi equations (Zhou and Garcia-Bennett, 2010). These parameters are shown in Table 3.

Drug release data are frequently plotted as percent (or fractional) drug released versus $t^{1/2}$ using the Higuchi model. Here, we attempt to do the same, but with loading enzyme instead of releasing. A linear plot indicates a diffusional controlled drug release (Higuchi, 1961), the same curves were calculated fitting power law equation and they have also the same shape (data not shown). Hence, we can assume that the PPO immobilization into mesoporous materials is a diffusion controlled mechanism. Besides, the coefficients of correlation of each model are considerably high. Table 3 obtained shows that the time needed to incorporate 50% of PPO depends directly on the pore volume of the material. Materials with higher pore volume, such as Aeroperl® or SBA-15, need less than 1 min to incorporate the same quantity of enzyme as STA-11 does in 6 hours.

TABLE 3. Parameters of power law and Higuchi equations for the loading curves of PPO loading into mesoporous materials at pH 4.00.

	Power law: $\ln F = \ln k_p + n \ln t$			Higuchi: $F = k_H t^{1/2}$		
	k_p	n	R	k_H	R	$T_{50\%}$ (min)
Aeroperl	0.58	0.02	0.95	0.03	0.89	0.17
SBA-15	0.87	0.01	1.00	0.02	0.97	0.10
SBA-3	0.28	0.32	0.99	0.27	0.80	18.04
MCM-48	0.76	0.37	0.99	0.74	0.91	131.32
STA-11	1.29	0.41	0.94	1.27	0.92	390.21

k_p: kinetic constant; n: loading exponent; R: coefficient of correlation; $T_{50\%}$: the time loaded 50% of PPO.

In situ ACTIVITY ASSAYS

After testing the materials with model solutions, activity assays were done with apple extract containing PPO enzyme. The initial activity was measured and stablished for time 0 in 405 U·mg^{-1} and 608 U·mg^{-1} for the two extract samples used, according with the enzymatic activity units stablished in Guerrero, 2009. Then, the variation in the activity was observed at different times for one hour.

Figure 11 shows the results of the assays. The activity decreases by more than half of the initial activity in the case of the Aeroperl® material after one hour of immobilization reaction. Furthermore, with this material after 30 min of immobilization assay, the extract experienced an activity fall of 61%, after which it remained constant. In the case of SBA-15, the activity reduced to 63% after 30 min, but surprisingly increased to 71% after that period. One possible explanation is that the material can retain and adsorb the PPO in a short period of time (30 min) but PPO may not be de-natured within the pores. Finally, STA-11 reduced the initial activity of the extract to 62% during the first 15 min and it remains almost constant after 45 min.
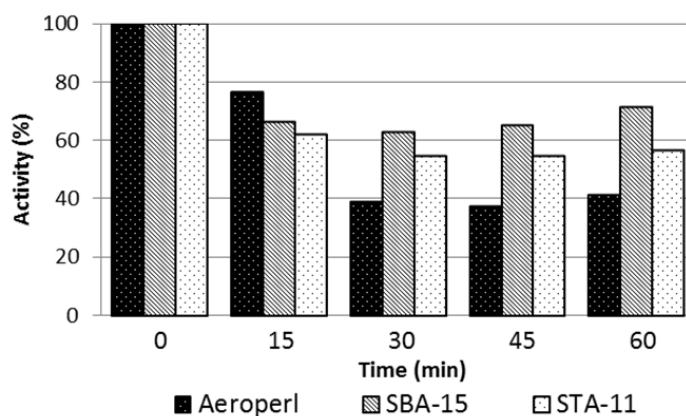
FIGURE 11. Enzymatic activity measured for one hour.

This last result is unexpected, since STA-11 was used as a negative control. This material was chosen because *in vitro* immobilization assays showed a lower quantity of immobilized PPO. The activity assays suggests that even though the material cannot immobilize PPO, it can inhibit or decrease its activity.

CONCLUSIONS

From the characterization analysis, we can conclude that all the materials used have different structure, morphology and textural properties. Some of them present microporosity (SBA-15 and STA-11) and others do not but all of them have a narrow pore size distribution. The three main factors which most influence the quantity of enzyme immobilized by mesoporous materials are the pH value, its pore volume and exposure time. A pH value of 4.00 offers higher immobilization rate followed by the values nearby (3.00 and 5.00) because the electrostatic interactions are favorable between the enzyme and the silanol groups of the mesoporous walls. The influence of pH in the amount of PPO adsorbed is considerably more for materials with higher pore volume, such as Aeroperl® and SBA-15. These materials also need less time to reach their maximum quantity of PPO adsorbed in their walls. Fitting power law and Higuchi models verify that this protein goes into the pores by diffusion. The initial activities of the two apple extracts analysed vary considerably between samples. Aeroperl®, after half hour of immobilization assay, is capable of reducing the browning reaction by more than 60% of its initial value. The materials behave differently from model solutions to real apple extracts.

FUTURE WORK

This work has studied the possibility to apply mesoporous silica materials for the entrapment of polyphenol oxidase which causes large economic losses in the horticultural industry. I feel that an important point to make is to improve the properties of the food and beverages available nowadays in the market. Removing this enzyme without adding any additives or any heating treatment, from my point of view, is very satisfactory because it can offer consumers the same products but with added nutritional value.

The full understanding of the uptake mechanism of immobilizing food enzymes in mesoporous silica particles and their interactions is required. It is necessary in order to broaden horizons in the field of porous materials. Specially, future studies should focus not only on how to improve the percentage of activity inhibition, but also knowing deeply the factors which affect this inhibition rate. In order to see if it is possible the application of this kind of materials in food science, we showed promising results of the use mesoporous particles as supports to retain PPO and decrease its activity which is the main reason for browning reactions in fruits and vegetables.

ACKNOWLEDGEMENTS

REFERENCES

Arroyo, M. 1998. Inmovilización de Enzimas. Fundamentos, Métodos y Aplicaciones. *Ars Pharmaceutica*, **39**(2):23-39.

Atluri, R. 2010. Novel Syntheses, Structures and Functions of Mesoporous Silica Materials. Doctoral Thesis in Engineering Sciences, Nanotechnology and Functional Materials at Uppsala University, Sweden. IBSN 978-91-554-7786-8.

Bagshaw, S.A., Prouzet, E., Pinnavaia, T.J. 1995. Templating of Mesoporous Molecular Sieves by Nonionic Polyethylene Oxide Surfactants. *Science*, **269**(5228):1242-1244.

Bradford, M.M. 1976. A Rapid and Sensitive Method for the Quantitation of Microgram Quantities of Protein Utilizing the Principle of Protein-Dye Binding. *Analytical Biochemistry*, **72**(1):248-254.

Brunauer, S., Emmett, P.H., Teller, E. 1938. Adsorption of Gases in Multimolecular Layers. *Journal of the American Chemical Society*, **60**(2):309-319.

Coseteng, M.Y., Lee, C.Y. 1987. Changes in Apple Polyphenoloxidase and Polyphenol Concentrations in Relation to Degree of Browning. *Journal of Food Science*, **52**(4):985-989.

Datta, S., Christena, L.R., Rajaram, Y.R.S. 2013. Enzyme Immobilization: an Overview on Techniques and Support Materials. *3 Biotech*, **3**(1):1-9.

Denoya, G.I., Ardanaz, M., Sancho, A.M., Benítez, C.E., González, C., Guidi, S. 2012. Efecto de la Aplicación de Tratamientos Combinados de Aditivos sobre la Inhibición del Pardeamiento Enzimático en Manzanas Cv. Granny Smith Mínimamente Procesadas. *Revista de Investigaciones Agropecuarias*, **38**(3):263-267.

Edler, K.J. 2011. Mesoporous Silicates. In: Bruce, D.W., O´Hare, D, Walton, R.I. (eds). *Porous Materials*. John Wiley & Sons, Ltd, Publication, United Kingdom, 69-145.

Fan, Y., Flurkey, W.H. 2004. Purification and Characterization of Tyrosinase from Gill Tissue of Portabella Mushrooms. *Phytochemistry*, **65**(6):671-678.

Gacche, R.N., Zore, G.B., Ghole, V.S. 2003. Kinetics of Inhibition of Polyphenol Oxidase Mediated Browning in Apple Juice by B-Cyclodextrin and L-Ascorbate-2-Triphosphate. *Journal of Enzyme Inhibition and Medicinal Chemistry*, **18**(1):1-5.

Giraldo, L.F., López, B.L., Perez, L., Urrego, S., Sierra, L., Mesa, M. 2007. Mesoporous Silica Applications. *Macromolecular Symposia*, **258**(1):129-141.

Han, L. 2010. Synthesis and Characterization of Functionalized Silica Mesoporous Crystals. Doctoral Thesis in Chemistry at Stockholm University, Sweden. ISBN 978-91-7447-029-1.

Hertog, M.G., Hollman, P.C., Katan, M.B. 1992. Content of Potentially Anticarcinogenic Flavonoids of 28 Vegetables and 9 Fruits Commonly Consumed in the Netherlands. *Journal of Agricultural and Food Chemistry*, **40**(12):2379-2383.

Higuchi, T. 1961. Rate of Release of Medicaments from Ointment Bases Containing Drugs in Suspension. *Journal of Pharmaceutical Sciences*, **50**(10):874-875.

Hodgkins, R.P., Garcia-Bennett, A.E., Wright, P. A. 2005. Structure and Morphology of Propylthiol-Functionalised Mesoporous Silicas Templated by Non-Ionic Triblock Copolymers. *Microporous and Mesoporous Materials*, **79**(1):241-252.

Huang, M.H., Dunn, B.S., Zink, J.I. 2000. *In situ* Luminescence Probing of the Chemical and Structural Changes During Formation of Dip-Coated Lamellar Phase Sodium Sol-Gel Thin Films. *Journal of the American Chemical Society,* **122**(15):3739-3745.

Inagaki, S., Fukushima, Y., Kuroda, K. 1993. Synthesis of Highly Ordered Mesoporous Materials from a Layered Polysilicate. *Journal of the Chemical Society, Chemical Communication*, (8), 680-682.

Kresge, C.T., Leonowicz, M.E., Roth, W.J., Vartuli, J.C, Beck, J.S. 1992. Ordered Mesoporous Molecular Sieves Synthesized by a Liquid-Crystal Template Mechanism. *Nature*, **359**(6397):710-712.

Kupferschmidt, N., Csikasz, R. I., Ballell, L., Bengtsson, T., Garcia-Bennett, A. E. 2014. Large Pore Mesoporous Silica Induced Weight Loss in Obese Mice. *Nanomedicine*, (0):1-9.

Lastoskie, C., Gubbins, K.E., Quirke, N. 1993. Pore Size Distribution Analysis of Microporous Carbons: a Density Functional Theory Approach. *The Journal of Physical Chemistry*, **97**(18):4786-4796.

Lü, Z.R., Shi, L., Wang, J., Park, D., Bhak, J., Yang, J.M., Park, Y., Zhou, H., Zou, F. 2010. The Effect of Trifluoroethanol on Tyrosinase Activity and Conformation: Inhibition Kinetics and Computational Simulations. *Applied Biochemistry and Biotechnology*, **160**(7):1896-1908.

Mangrulkar, P.A., Yadav, R., Meshram, J.S., Labhsetwar, N.K., Rayalu, S.S. 2012. Tyrosinase-Immobilized MCM-41 for the Detection of Phenol. *Water, Air & Soil Pollution*, **223**(2):819-825.

Marín-Zamora, M.E., Rojas-Melgarejo, F., García-Cánovas, F., García-Ruiz, P.A. 2009. Production of *o*-Diphenols by Immobilized Mushroom Tyrosinase. *Journal of Biotechnology*, **139**(2):163-168.

Murata, M., Noda, I., Homma, S. 1995. Enzymatic Browning of Apples on the Market: Relationship between Browning, Polyphenol Content, and Polyphenol Oxidase. *Nippon Shokuhin Kogyo Gakkai-Shi*, **42**(10):820-826.

Olivas, G.I., Mattinson, D.S., Barbosa-Cánovas, G.V. 2007. Alginate Coatings for Preservation of Minimally Processed 'Gala' Apples. *Postharvest Biology and Technology*, **45**(1):89-96.

Pérez-Esteve, E., Bernardos. A., Martínez-Mánez, R., Barat, J.M. 2013. Nanotechnology in the Development of Novel Functional Foods or their Package. An Overview Based in Patent Analysis. *Recent Patents on Food, Nutrition & Agriculture*. **5**(1):35-43.

Perez-Gago, M.B., Serra, M., Del Rio, M.A. 2006. Color Change of Fresh-Cut Apples Coated with Whey Protein Concentrate-Based Edible Coatings. *Postharvest Biology and Technology*, **39**(1):84-92.

Rocha, A.M.C.N., Morais, A.M. 2001. Influence of Controlled Atmosphere Storage on Polyphenoloxidase Activity in Relation to Colour Changes of Minimally Processed "Jonagored" Apple. *International Journal of Food Science and Technology*, **36**(4):425-432.

Sapers, G.M. 1993. Browning of Foods: Control by Sulfites, Antioxidants, and Other Means. *Food Technology*, **47**(10):75-84.

Schumacher, K., Ravikovitch, P.I., Du Chesne, A., Neimark, A.V., Unger, K.K. 2000. Characterization of MCM-48 Materials. *Langmuir*, **16**(10):4648-4654.

Sendovski, M., Kanteev, M., Ben-Yosef, V.S., Adir, N., Fishman, A. 2011. First Structures of an Active Bacterial Tyrosinase Reveal Copper Plasticity. *Journal of Molecular Biology*, **405**(1):227-237.

Smith, P.K., Krohn, R.I., Hermanson, G.T., Mallia, A.K., Gartner, F.H., Provenzano, M., Fujimoto, E.K., Goeke, N.M., Olson, B.J., Klenk, D.C. 1985. Measurement of Protein Using Bicinchoninic Acid. *Analytical Biochemistry*, **150**(1):76-85.

Taguchi, A., Schüth, F. 2005. Ordered Mesoporous Materials in Catalysis. *Microporous and Mesoporous Materials*, **77**(1):1-45.

Tanev, P.T., Pinnavaia, T.J. 1995. A Neutral Templating Route to Mesoporous Molecular Sieves. *Science*, **267**(5199):865-867.

Toribio, J.L., Lozano, J.E. 1986. Heat Induced Browning of Clarified Apple Juice at High Temperatures. *Journal of Food Science*, **51**(1):172-175.

Walker, J.R.L. 1964. Studies on the Enzymic Browning of Apples II. Properties of Apple Polyphenoloxidase. *Australian Journal of Biological Sciences*, **17**(2):360-371.

Wang, Y., Caruso, F. 2005. Mesoporous Silica Spheres as Supports for Enzyme Immobilization and Encapsulation. *Chemistry of Materials*, **17**(5):953-961.

Whitaker, J.R., Lee, C.Y. 1995. Recent Advances in Chemistry of Enzymatic Browning: an Overview. *Enzymatic Browning and Its Prevention*. ACS Symposium Series; American Chemical Society: Washington, DC, 2-7.

Yanagisawa, T., Shimizu, T., Kuroda, K., Kato, C. 1990. The Preparation of Alkyltrimethylammonium-Kanemite Complexes and their Conversion to Microporous Materials. *The Bulletin of the Chemical Society of Japan*, **63**(4):988-992.

Yokoi, T., Karouji, T., Ohta, S., Kondo, J. N.,Tatsumi, T. 2010. Synthesis of Mesoporous Silica Nanospheres Promoted by Basic Amino Acids and Their Catalytic Application. *Chemistry of Materials*, **22**(13):3900-3908.

Zhao, D., Feng, J., Huo, Q., Melosh, N., Fredrickson, G.H., Chmelka, B.F., Stucky, G.D. 1998. Triblock Copolymer Syntheses of Mesoporous Silica with Periodic 50 to 300 Angstrom Pores. *Science*, **279**(5350):548-552.

Zhou, C., Garcia-Bennett, A. E. (2010). Release of Folic Acid in Mesoporous NFM-1 Silica. *Journal of Nanoscience and Nanotechnology*, **10**(11):7398-7401.